ELECTRONIC STRUCTURE AND PROPERTIES OF POLYNUCLEAR AROMATIC KETONES AND QUINONES. I. ELECTRONIC SPECTRA AND π-ELECTRONIC STRUCTURE OF SOME POLYNUCLEAR QUINONES

M.Titz and M.Nepraš

*Research Institute for Organic Syntheses, Pardubice-Rybitví*

The results of the theoretical and experimental study on six polynuclear quinones are presented. In calculations on the electronic spectra a variable $\beta_{\mu\nu}^{core}$ approximation was adopted. A detailed parametrization study for the C=O bond was performed. It was found impossible to interpret the electronic transitions of *para*, *ortho*, and *peri*-condensed quinones by means of one set of parameters. On varying the parameter b which concerns the C=O bond, a bond alternation and crossing of SCF electronic levels was inspected. For the bands of 9,10-phenanthrenequinone and 3,10-pyrenequinone we present the experimental data on polarization directions, obtained from electric dichroism measurements.

In accordance with the computational possibilities the simple MO LCAO method[1-3] was the only method used for estimations of spectral behaviour of quinones until the late fifties. This method was used by Koutecký and coworkers[4] in the study on 43 symmetrical quinones. Later a more complex, but more advanced SCF MO LCI method[5-8] (PPP) was employed, predominantly for estimations of spectral behaviour. In all these calculations a trouble was encountered how to take into consideration a lone pair on oxygen which is responsible for the longest-wavelength n-π^* band. Anno and collaborators[9-11] solved this problem on somewhat inconsistent grounds as well as the authors who applied[12-14] this method. Combining the concepts of Sandorfy[15], Yoshizumi[16], and Hoffmann[17], Yonezawa[18] developed a method which permits to treat this problem in the one-electron approach. However, the satisfactory and consistent results were not obtained before the CNDO CI method was employed, as shown by Leibovici for *p*-benzoquinone[19]. Nevertheless in the last years the attention has again been paid to the π-electronic structure of quinones[20-22] when the variable β and γ approximations were introduced[23] into the PPP method. The stimulus for these attempts arose from the paper of Nishimoto and Forster[21], who employed a variable β approximation. Following their procedure successful results were obtained not only for benzenoid hydrocarbons and their derivatives[24] but also for nonbenzenoid aromatic systems[22,25]. A particularly interesting paper was published by Kunii and Kuroda[20], who adopted both β and γ approximation and by means of the PPP method modified in this way studied 35 quinones and aromatic hydroxy derivatives.

We used the LCI SCF MO (PPP) method with the variable β approximation and calculated the theoretical spectra of *p*-benzoquinone, 1,4-naphthoquinone, 9,10-anthraquinone, 9,10-phenanthrenequinone, 3,10-pyrenequinone, and 3,8-pyrenequinone. This series is obviously inhomogeneous since four representants are derived

from *cata*-condensed hydrocarbons and the remaining two are derived from *peri*-condensed hydrocarbons. Even the group of *cata*-condensed quinones alone is inhomogeneous, since 9,10-phenanthrenequinone is an *ortho* quinone while the other
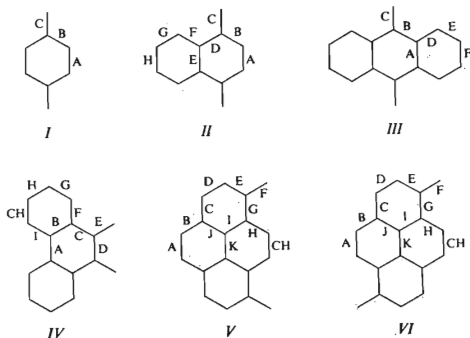
SCHEME 1

three are *para* quinones. Moreover, the position of *p*-benzoquinone is similarly special as that of benzene in the series of benzenoid hydrocarbons. The choice of this series of compounds was dictated by the experimental accessibility and by available results of electric dichroism measurements for 9,10-phenanthrenequinone and 3,10-pyrenequinone, which permit to interpret the absorption spectra in more detail.

In this paper we attempted to find whether the same set of parameters can be used for quinones of various types in spite of the known dependence of $\beta_{\mu\nu}^{core}$ on the size of molecules.

CALCULATIONS

In calculations of spectral characteristics we employed the LCI SCF MO method with the variable β^{core} approximation. For all six molecules we assumed the usual regular geometry with all angles and the C—C bond lengths being 120° and 1·40 Å, respectively. The C=O bond length was fixed[26] at 1·15 Å (found for *p*-benzoquinone and 9,10-anthraquinone). In more recent papers a somewhat higher value (1·22 Å) was reported[27,28] but regarding a semiempirical nature of this method the respective difference is believed to be negligible.

Two-centre core integrals were reevaluated in each iteration by means of the following relationship

$$\beta_{\mu\nu}^{core} = \beta_{\mu\nu}^{(0)} \cdot 0\cdot8 \cdot \exp\left(\alpha \cdot p_{\mu\nu}\right), \tag{1}$$

where

$$\beta_{\mu\nu}^{(0)} = -2\cdot318 \text{ eV} \quad \text{for the C—C bond .}$$

For the C=O bond we assumed

$$\beta_{C=O}^{(0)} = b \cdot \beta_{C-C}^{(0)} = b(-2\cdot318) , \tag{2}$$

where b was chosen as $1\cdot1$ on grounds of the parametrization study. In Eq. (*1*) $p_{\mu\nu}$ stands for the bond order of the bond between the atoms μ and ν. Instead of a linear relationship used for the variable β^{core} approximation in paper[20–22,24,25] we adopted the exponential relationship, which was used in papers[29,30] and verified in detail by Hochmann[31]. We assumed the same value $\alpha = = 0\cdot335$ both for C—C and C=O bonds, because the transition energies were found to be dependent very little on this parameter.

One-centre repulsion integrals, $\gamma_{\mu\mu}$, were calculated by means of the Pariser's approximation[32]

$$\gamma_{\mu\mu} = I_\mu - A_\mu , \tag{3}$$

where I_μ and A_μ is the ionization potential and electron affinity of the atom μ (both values for the corresponding valence states). Hence the following values for γ_{cc} and γ_{00} were adopted:

$$\gamma_{cc} = 11\cdot42 - 0\cdot58 = 10\cdot84 \text{ eV} ,$$

$$\gamma_{00} = 17\cdot70 - 2\cdot47 = 15\cdot23 \text{ eV} .$$

Two-centre repulsion integrals, $\gamma_{\mu\nu}(\mu \neq \nu)$ were evaluated according to the Nishimoto and Mataga approximation[33].

EXPERIMENTAL

9,10-Phenanthrenequinone was prepared by oxidation of phenanthrene with chromium trioxide in sulfuric acid[34]. M.p. 209°C corr.(lit.[34] 208·5–210°C corr.) 3,8- and 3,10-pyrenequinones were prepared by oxidation of pyrene with chromium trioxide in acetic acid and separated from the oxidation mixture chromatographically on a thin layer of Al_2O_3 (with 10% H_2O, washed by benzene)[35]. Products were chromatographically homogeneous. Dioxane and methanol were purified in the usual way[36].

Spectra of *p*-benzoquinone, 1,4-naphthoquinone, 9,10-anthraquinone, and 9,10-phenanthrenequinone were taken from the literature[37]. Spectra of 3,10-pyrenequinone and 9,10-phenanthrenequinone were measured on a Zeiss PMQ II spectrophotometer, the spectra of both pyrenequinones in methanol were recorded on Unicam SP 700 spectrophotometer.

Electrooptical absorption measurements were performed on the apparatus described elsewhere[38]. Molecules having a permanent dipole moment or an anisotropic polarizability in their ground states are oriented in an external static electric field and the absorption measurements with a linear polarized light permit to determine the directions of transition moments and some other important molecular characteristics in the ground and excited states[39–41]. The apparatus mentioned[38] permits to measure directly the values of q_χ if the incident light is perpendicular to the direction of the external electric field and if χ is the angle between the polarization plane of the incident light and the direction of the external field. From q_χ one can calculate the quantity L_χ' by means of the relationship[41]

$$L'_\chi = -\frac{q_\chi}{2 \cdot 303 \cdot D \cdot F_e^2} = -\frac{1}{2 \cdot 303 \cdot D \cdot F_e^2} \cdot \frac{I_\chi - I_{\chi(F_e = 0)}}{I_{\chi(F_e = 0)}}, \qquad (4)$$

where D is the extinction of the solution at the wavenumber $\tilde{v}_a$ without an external field and in a natural light, F_e is a field strength at the location of the molecule depending on the external field parameters and on the dielectric constant of the solvent, I_χ is the intensity of the light transmitted through the solution exposed to a homogeneous external field, $I_{\chi(F_e = 0)}$ is the same quality in absence of the external field. For a separated absorption band L'_χ depends on χ and on $\tilde{v}_a$[41]. From the dependence of L'_χ on $(d\ln(\varepsilon/\tilde{v})/d\tilde{v})_{\tilde{v}_a}$ the values of A_χ and B_χ[38,41,42] can be obtained. The dependence of A_χ and B_χ on χ permits to determine quantities D, E, F, G depending on the properties of the solvent and the solute[38,42] (Table I). The experimental data were treated by the procedure described elsewhere[38,41–43].

RESULTS

Dependence of LCI Transition Energies on the Parameter b

Dependences of the eight lowest $\pi\pi^*$ transition energies of the quinones studied on the parameter b are presented in Figs 1—6. On the y-axis we have the energy scale in eV for the transition energies; the experimental transition energies are indicated by thick horizontal lines. Allowed transitions are indicated by thin full lines together with the marks characterising the polarization of the transition: $\perp$ for sin (P, X) = 1; $//$ for sin (P, X) = 0; (the X-axis is denoted in a schematic formula of the molecule Fig. 7). Forbidden transitions are indicated by dashed lines. Numbers at the individual points denote the main configuration.

On going from lower to higher values of the parameter b, *i.e.* from lower to higher values of $\beta^{core}_{C=O}$, the transition energy becomes higher. Curves of these dependences have a different slope, which lowers as a size of the molecule enlarges. In the plots of transition energies against b (Figs 1—6) the change of the main configuration occurs several times. The reason for it can be either a dependence of the π-electronic Hamiltonian matrix elements in the basis of singly excited configurations on the parameter b leading to an interchange of two configurations with comparable weights or a crossing of the SCF molecular orbital levels. With p-benzoquinone a crossing of unoccupied SCF molecular orbitals 2' and 3' occurs in the interval (0·7; 0·8) of b. With 1,4-naphthoquinone a crossing of occupied levels 4 and 5 in the interval (0·9; 1·0) of b does not lead to a change of main configurations in the eight lowest excited states. The dependence of the SCF molecular orbitals of 9,10-anthraquinone on the parameter b is rather complex. In the interval (0·8; 0·9) a crossing of unoccupied levels 5' and 6' occurs, which has no effect on the main configuration in the eight lowest excited states. The other crossings are the following: in the interval (0·9; 1·0) occupied levels 2 and 3 and in the interval (1·0; 1·2) occupied levels 4,2 and 6,7. With 9,10-phenanthrenequinone crossings of unoccupied levels 2' and 3' and occupied levels 6 and 7 in the interval (1·0; 1·2) are observed. With 3,10-pyrene-quinone only crossings of occupied occur: levels 3 and 4 in the interval (0·7; 0·8) and

level 2 in the interval $(0.8; 0.9)$ crosses both 3 and 4. In the SCF MO level scheme for 3,8-pyrenequinone only a crossing of occupied levels 6 and 7 occurs in the interval $(1.0; 1.2)$, which does not affect the first eight transitions.

Electronic spectra of six quinones under study are presented in Fig. 7. The arrow in formulas of molecules represents the axis to which the polarization detections of theoretical and known experimental transition moments are related. The thick vertical lines indicate allowed transitions, the short wavy lines the forbidden ones. The parameter b is taken 1.1 for all molecules studied.

In order to obtain an agreement between the experimental and theoretical transition energies for first two $\pi\pi^*$ absorption bands of p-benzoquinone the parameter b should be greater than 1.2, as seen in Fig. 1. A similar fit for 1,4-naphthoquinone (Fig. 2) requires b to lie in the interval $(1.0; 1.2)$. Fig. 3 indicates the optimal b for 9,10-anthraquinone is 1.1. 9,10-Phenanthrenequinone is seen, in Fig. 4, to be the only representant of *ortho* quinones for which the most suitable value for b lies somewhat in the
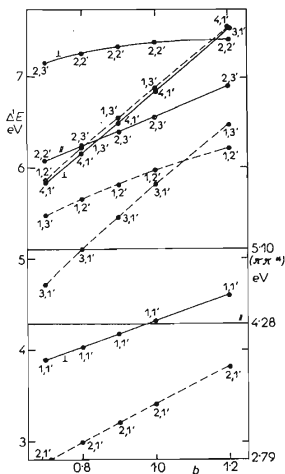

FIG. 1

Dependence of Singlet $\pi\pi^*$ Transitions on Parameter b for p-Benzoquinone

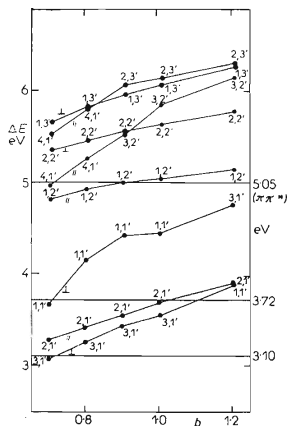Experimental data are indicated by thick lines.

FIG. 2

Dependence of Singlet $\pi\pi^*$ Transitions on Parameter b for 1,4-Naphthoquinone

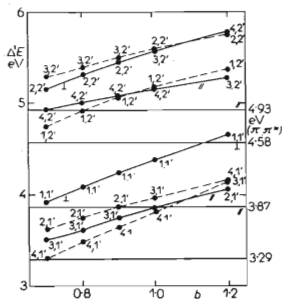Experimental data are indicated by thick lines.

FIG. 3

Dependence of Singlet $\pi\pi^*$ Transitions on Parameter b for 9,10-Anthraquinone

Experimental data are indicated by thick lines.

FIG. 4

Dependence of Singlet $\pi\pi^*$ Transitions on Parameter b for 9,10-Phenanthrenequinone

Experimental data are indicated by thick lines.
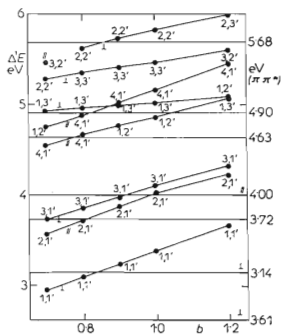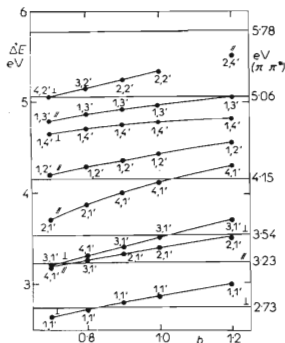

FIG. 5

Dependence of Singlet $\pi\pi^*$ Transitions on Parameter b for 3,10-Pyrenequinone

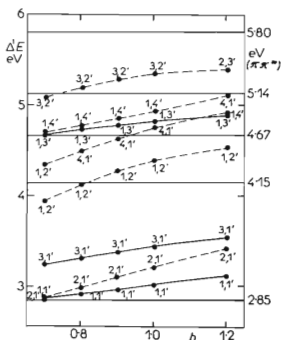Experimental data are indicated by thick lines.

FIG. 6

Dependence of Singlet $\pi\pi^*$ Transitions on Parameter b for 3,8-Pyrenequinone

Experimental data are indicated by thick lines.

interval (0·7; 0·9). With both pyrenequinones the choice of b is not ambiguous, since the transition energies are seen, in Figs 5 and 6, to be rather insensitive on the magnitude of b.

Theoretical characteristics for the eight energy lowest singlet $\pi\pi^*$ transitions are summarized in Table II. For three of the systems under study we present dependences of bond orders of the quinoid ring on b in Figs 8—10. The entries in Table III are the SCF bond orders calculated for b 1·1, calculated bond lengths $\left(r_{\mu\nu}^{SCF}(\text{Å}) = 1·517 - 0·180p_{\mu\nu}^{SCF}\right)^{44}$, and bond lengths determined from the X-ray analysis; for a comparison also the experimentally determined bond lengths for parent hydrocarbons are listed.
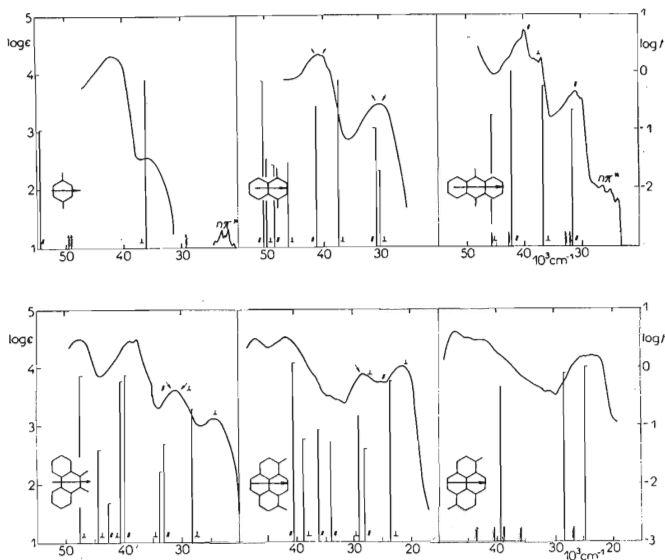

Fig. 7

Electronic Absorption Spectra of the Quinones Studied

Allowed transitions are indicated by thick vertical lines, forbidden ones by wavy line (for b 1·1); solvents used: methanol (for 1,4-naphthoquinone, 9,10-phenanthrenequinone, 3,10-pyrenequinone, and 3,8-pyrenequinone), hexane (for p-benzoquinone), cyclohexane (for 9,10-anthraquinone).

Electric Dichroism Measurements

Fig. 11 presents the absorption spectrum of phenanthrenequinone measured in dioxane, wavenumber dependence of L' for $\chi = 0°$, $54.7°$, $90°$, and wavenumber dependence of δ' (and γ' respectively)[41,45]. In the region $19\,000 - 21\,000$ cm^{-1} there is a weak band which is probably due to a $n\pi^*$ transition. Shapes of the wavenumber dependences of L'_χ and $\delta'(\gamma')$ indicate[41] the direction of the respective transition moment is perpendicular to the direction of the dipole moment and the excitation leads to a decrease in the dipole moment. The theoretical data for this band, however, are missing in our study. In the region $23\,000 - 27\,000$ cm^{-1} a moderately strong band is observed arising from the first $\pi\pi^*$ electronic transition. From the L'_χ and δ' curves it appears the respective transition moment is perpendicular to the direction of the dipole moment μ_g and the excitation leads to the increase in the dipole moment.

TABLE I

Electrooptical Absorption Measurements[a] on 9,10-Phenanthrenequinone in Dioxane at 20°C

Quantity	Magnitude	Quantity	Magnitude
$\tilde{\nu}_{max}$ (10^3 cm^{-1})	25·3	$G . 10^{21}$	$-\ 1·45 \pm 0·37$
$\log \varepsilon_{max}$	3·26	$\gamma' . 10^{10}$	-80
Interpreted region (10^3 cm^{-1})	23·4 — 26·0	$\alpha_g . 10^{24}$	19·5
$(\varepsilon_{DK})_{solv.}$	2·21	a (Å) (from model)	3·5
$(f_e)^2_{solv.}$	1·40	$(1 - f\alpha_g)$	$0·86 \pm 0·04$
$(n^2)_{solv.}$	2·03	Irred. repres.	B_2
Number of iterations	2	μ^2 from $\gamma' . 10^{36}$	$28·10 \pm 0·43$
$A_0 . 10^{10}$	$-17·19 \pm 0·51$	$\mu^2 . 10^{36}$ (calc. from E)	$27·57 \pm 1·69$
$A_{54·7} . 10^{10}$	$-\ 1·48 \pm 0·45$	$\mu^2 . 10^{36}$ (best value)	$28·10 \pm 0·43$
$A_{90} . 10^{10}$	$6·55 \pm 0·37$	$(\mu . \Delta\mu) . 10^{35}$ (calc. from F)	$3·53 \pm 2·0$
$B_0 . 10^{21}$	$3·22 \pm 0·39$	$\mu . 10^{18}$ (best value)	$5·30 \pm 0·66$
$B_{54·7} . 10^{21}$	$6·11 \pm 0·36$	$(\mu . \Delta\mu) . 10^{35}$ (calc. from G)	$4·19 \pm 1·07$
$B_{90} . 10^{21}$	$7·78 \pm 0·30$	$(\mu . \Delta\mu) . 10^{35}$ (best value)	$3·53 \pm 0·20$
$D . 10^{10}$	$-\ 4·44 \pm 1·35$	$\Delta\mu . 10^{18}$	$6·66 \pm 1·21$
$E . 10^9$	$-23·54 \pm 1·44$	$(\mu_a - \mu_g) . 10^{18}$	$5·7 \pm 1·2$
$F . 10^{21}$	$1·22 \pm 0·07$	$\mu_g . 10^{18}$	$4·5 \pm 0·2$
		$\mu_a . 10^{18}$	$10·3 \pm 1·4$

[a] The highest values of $\left[\left(\dfrac{d \ln \varepsilon/\tilde{\nu}}{d\tilde{\nu}} \right)^2_{\tilde{\nu}_a} + \left(\dfrac{d^2 \ln \varepsilon/\tilde{\nu}}{d\tilde{\nu}^2} \right) \right]$ in the region $23\,400 - 26\,000$ cm^{-1} are of magnitude $3 . 10^{-7}$ and the expression $\dfrac{1}{30h^2c^2} \left[\left(\dfrac{d \ln \varepsilon/\tilde{\nu}}{d\tilde{\nu}} \right)^2_{\tilde{\nu}_a} + \left(\dfrac{d^2 \ln \varepsilon/\tilde{\nu}}{d\tilde{\nu}^2} \right) \right] C$ amounts to $0·64 . 10^{10}$. This implies that the value lies in the range of experimental errors.

As in the region $23\,500 - 26\,000$ cm^{-1} this band does not overlap with another band (γ' is nearly constant) it was possible to interpret the electrooptical measurements in this region following the procedure of Liptay and coworkers[41,43]. The results are given in Table I. The direction of the transition moment follows from the value of E^{41}, the change in the dipole moment from the values of F and G^{41}. Electrooptical measurements give the value $\mu_g = 4.5 \pm 0.2$ D for the dipole moment in the ground state. The value reported in the literature[46] for the same compound, $\mu_g = 5.66$ D, was determined from the dielectric measurements in dioxane. For $\Delta\mu$ measured electrooptically the value 5.7 ± 1.2 D was found. The calculated μ_a is 10.3 ± 1.4 D and 11.5 D considering for μ_g the value found electrooptically and from dielectric measurements, respectively. The agreement is very good.

The other bands could not be treated in this way owing to their considerable overlapping. The curves of L'_χ and δ' permit only to judge that in the region $28\,000$ to $35\,000$ cm^{-1} there are two considerably overlapped bands with parallel transition moments, the longer-wavelength band being connected with a decrease and the shorter-wavelength band with an increase in the dipole moment upon excitation.

Fig. 12 presents the absorption spectrum and the wavenumber dependences of L'_χ and γ' (δ') for 3,10-pyrenequinone. The interpretation of the experimental data could not be done owing to a considerable band overlapping in the whole measured
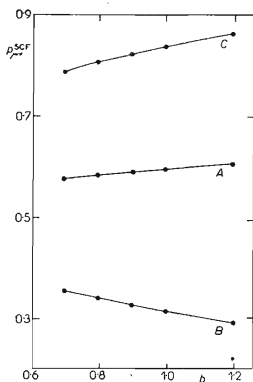

FIG. 8

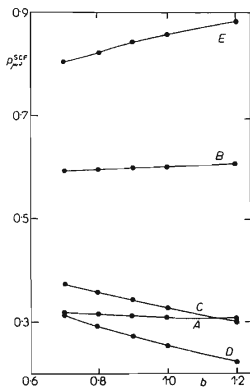Dependence of the SCF Bond Order on Parameter b for 9,10-Anthraquinone

FIG. 9

Dependence of the SCF Bond Order on Parameter b for 9,10-Phenanthrenequinone

spectral region. From the nature of the absorption spectrum and the L'_χ and $\gamma'(\delta')$ curves one can deduce only that in the region $20\,000-24\,000$ cm^{-1} there are several overlapping bands with transition moments perpendicular to the molecular dipole moment. The same polarization direction and low energy differences indicate these bands are a vibration structure of one electronic transition. A possible interpretation of the shape of the L'_χ curve in the region $25\,000-30\,000$ cm^{-1} could be a presence of two overlapping bands with the mutually perpendicular electronic transitions, the polarization direction of the longer-wavelength band being parallel to the molecular dipole moment.

DISCUSSION

In the series of three *para* quinones the least satisfactory correspondence between theory and experiment was found for *p*-benzoquinone. This special position of *p*-benzoquinone is due to its most outstanding bond length alternation in the series of poly-nuclear quinones. In the spectrum of *p*-benzoquinone in the region $20\,000-25\,000$ cm^{-1} there is a $n\pi^*$ band, which is not interpreted by the method employed. The
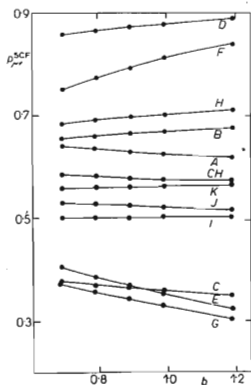

FIG. 10

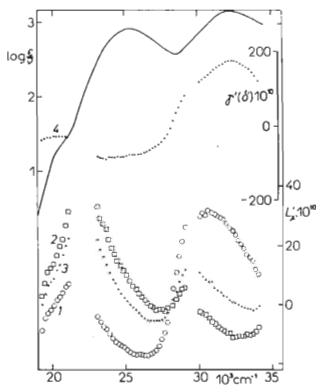Dependence of the SCF Bond Order on Parameter b for 3,10-Pyrenequinone

FIG. 11

Absorption Spectrum and Electrooptical Data on 9,10-Phenanthrenequinone in Dioxane at 20°C

1 $L'_{\chi=0^\circ}$, 2 $L'_{\chi=90^\circ}$, 3 $L_{\chi=54.7^\circ}$, 4 $\gamma'(\delta')$.

TABLE II

Theoretical Characteristics of Singlet Transitions for $b\,1{\cdot}1$

Meaning of symbols: P_x, P_y is the x and y component of the transition moment vector, $\sin(P, X)$ is the angle between the transition moment vector and a positive direction of the x-axis, V_{ij} (in eV) is the diagonal element in the basis of singlet functions and $\Delta\varepsilon_{HF}^{ij}$ (eV) is the energy difference between the Hartree–Fock levels i and j.

Quantity	p-Benzoquinone	1,4-Naphtho-quinone	9,10-Anthra-quinone	9,10-Phenan-threnequinone	3,10-Pyrene-quinone	3,8-Pyrene-quinone
Δ^1E_1 (eV)	3·615	3·727	3·958	3·507	2·926	3·063
P_x	—	0·000	0·800	0·000	0·000	0·638
P_y	—	0·247	0·000	0·799	1·574	1·704
$\sin(P, X)$	—	0·00	0·00	1·00	1·00	0·93
$\log f$	—	−1·677	−0·642	−0·700	−0·189	−0·052
Main configuration	2·1′ (99·13)	3·1′ (54·10)	2·1′ (83·96)	1·1′ (97·60)	1·1′ (94·30)	1·1′ (93·15)
Next significant configuration	—	1·1′ (42·97)	—	—	—	—
V_{ij} (eV)	3·654	4·208	4·162	3·493	3·044	3·182
$\Delta\varepsilon_{HF}^{ij}$ (eV)	7·443	7·345	7·193	6·468	5·298	5·297
Δ^1E_2 (eV)	4·455	3·803	3·980	4·104	3·447	3·324
P_x	0·000	0·568	—	0·380	1·385	—
P_y	1·447	0·000	—	0·000	0·000	—
$\sin(P, X)$	1·00	0·00	—	0·00	0·00	—
$\log f$	−0·092	−0·968	—	−1·312	−1·344	—
Main configuration	1·1′ (90·79)	2·1′ (87·25)	3·1′ (97·74)	2·1′ (68·92)	2·1′ (78·23)	2·1′ (95·66)
Next significant configuration	—	—	—	1·3′ (21·93)	—	—
V_{ij} (eV)	4·735	3·978	4·018	4·400	3·800	3·387
$\Delta\varepsilon_{HF}^{ij}$ (eV)	6·868	6·982	7·188	7·156	6·543	6·304
Δ^1E_3 (eV)	6·098	4·610	4·064	4·197	3·608	3·498
P_x	—	0·000		0·000	0·000	0·730

P_y	—	1·352	—	0·208	0·694	0·246
sin (P, X)	—	1·00	—	1·00	1·00	0·32
log f	—	—0·133	—	—1·790	—0·813	—0·742
Main configuration	1·2' (98·97)	1·1' (53·42)	4·1' (79·18)	3·1' (86·70)	3·1' (92·13)	3·1' (79·18)
Next significant configuration	—	3·1' (41·57)	—	—	—	1·3' (15·02)
V_{ij} (eV)	6·120	4·313	4·337	4·333	3·596	3·745
$\Delta\varepsilon_{HF}^{ij}$ (eV)	9·662	6·863	7·196	7·237	6·688	6·538
$\Delta^1 E_4$ (eV)	6·147	5·108	4·525	4·946	4·201	4·457
P_x	—	0·763	0·000	1·258	0·388	—
P_y	—	0·000	1·229	0·000	0·000	—
sin (P, X)	—	0·00	1·00	0·00	0·00	—
log f	—	—0·582	—0·214	—0·130	—1·254	—
Main configuration	1·3' (54·20)	1·2' (52·67)	1·1' (95·56)	1·3' (37·23)	4·1' (76·73)	1·2' (86·00)
Next significant configuration	3·1' (44·47)	2·3' (26·19); 2·1' (12·75)	—	2·1' (28·17); 2·2' (22·04)	1·3' (12·42)	—
V_{ij} (eV)	6·686	5·398	4·598	—	4·265	4·543
$\Delta\varepsilon_{HF}^{ij}$ (eV)	10·110	8·686	7·023	—	6·797	7·153
$\Delta^1 E_5$ (eV)	6·728	5·719	5·221	5·035	4·487	4·823
P_x	0·557	0·000	1·532	0·000	0·452	—
P_y	0·000	0·227	0·000	1·141	0·000	—
sin (P, X)	0·00	1·00	0·00	1·00	0·00	—
log f	—0·861	—1·790	—0·031	—0·230	—1·108	—
Main configuration	2·3' (97·90)	2·2' (67·39)	3·2' (61·76)	1·2' (82·31)	1·2' (74·62)	1·4' (50·99)
Next significant configuration	—	1·3' (31·44)	1·4' (15·77); 2·1' (14·31)	—	1·3' (20·59)	4·1' (41·07)
V_{ij} (eV)	6·772	5·883	5·442	5·065	4·563	4·917
$\Delta\varepsilon_{HF}^{ij}$ (eV)	10·694	8·820	8·536	8·963	7·095	7·849

Table II
(Continued)

Quantity	p-Benzoquinone	1,4-Naphtho-quinone	9,10-Anthra-quinone	9,10-Phenan-threnequinone	3,10-Pyrene-quinone	3,8-Pyrene-quinone
$\Delta^1 E_6$ (eV)	7·183	6·008	5·294	5·287	4·798	4·858
P_x	0·000	0·213	—	0·088	0·000	1·038
P_y	0·438	0·000	—	0·000	0·377	0·093
sin (P, X)	1·00	0·00	—	0·00	1·00	0·09
log f	−0·986	−1·790	—	−2·379	−1·214	−0·362
Main configuration	4·1' (74·91)	3·2' (54·60)	1·2' (59·59)	4·1' (81·60)	1·4' (97·92)	1·3' (75·80)
Next significant configuration	—	1·2' (28·80); 2·3' (12·87)	4·1' (19·46); 2·3' (12·39)	1·3' (14·22)	—	2·2' (13·02)
V_{ij} (eV)	7·333	6·097	5·438	5·267	4·808	4·740
$\Delta\varepsilon^{ij}_{\text{HF}}$ (eV)	10·678	9·175	8·359	8·038	7·778	7·705
$\Delta^1 E_7$ (eV)	7·198	6·179	5·683	5·522	5·007	5·021
P_x	—	0·000	—	0·000	1·658	—
P_y	—	0·422	—	0·278	0·000	—
sin (P, X)	—	1·00	—	1·00	0·00	—
log f	—	−1·042	—	−1·437	0·074	—
Main configuration	3·1' (54·07)	1·3' (60·38)	2·2' (74·93)	3·2' (45·23)	1·3' (55·61)	1·4' (45·13)
Next significant configuration	1·3' (44·22)	2·2' (26·42)	1·3' (16·51)	1·4' (26·86); 2·3' (13·83)	2·1' (15·26); 4·1' (12·80)	4·1' (39·91)
V_{ij} (eV)	6·682	6·082	5·795	—	4·680	—
$\Delta\varepsilon^{ij}_{\text{HF}}$ (eV)	10·114	9·190	8·538	—	7·650	—
$\Delta^1 E_8$ (eV)	7·393	6·245	5·685	5·894	5·426	5·374
P_x	0·000	1·161	0·000	0·000	0·000	—
P_y	1·387	0·000	0·588	1·203	0·169	—
sin (P, X)	1·00	0·00	1·00	1·00	1·00	—

TABLE IV

Characteristics of the First S–T Transition for b 1·1

Quantity	p-Benzoquinone	1,4-Naphthoquinone	9,10-Anthraquinone	9,10-Phenanthrenequinone	3,10-Pyrenequinone	3,8-Pyrenequinone
log f	0·093	−0·115	−0·757	−0·117	−1·825	—
Main configuration	2·2′ (78·12)	2·3′ (42·75)	4·2′ (83·36)	2·3′ (81·50)	2·2′ (98·93)	3·2′ (42·09)
Next significant configuration	—	3·2′ (30·23)	—	—	—	2·3′ (30·99); 3·4′ (17·21)
V_{ij}	7·260	—	5·767	5·838	5·404	—
$\Delta\varepsilon_{HF}$ (eV)	10·237	—	8·516	8·664	8·382	—
$\Delta^3 E_1$ (eV)	0·794	1·742	2·322	2·456	1·198	1·167
Main configuration	1·1′ (82·67)	1·1′ (51·16)	1·1′ (74·99)	1·1′ (64·98)	1·1′ (89·80)	1·1′ (89·82)
Next significant configuration	—	3·1′ (36·95)	—	3·1′ (17·69)	—	—
T_{ij} (eV)[a]	1·620	—	2·838	2·896	1·559	1·542
$\Delta\varepsilon_{HF}$ (eV)[b]	6·868	—	7·023	6·468	5·298	5·297

[a] Diagonal element in the basis of triplet functions. [b] $\Delta\varepsilon_{HF}^{ji}$ is the energy difference between Hartree–Fock levels i and j.

Table III

Comparison of Theoretical Bond Lengths (for b 1·1) in Quinones, r^{SCF} (Å), and Experimental Bond Lengths in Related Hydrocarbons, r^{exp} (Å)

Bond[a]	$p_{\mu\nu}^{SCF}$	$r_{\mu\nu}^{SCF}$	$r_{\mu\nu}^{exp}$	Bond[a]	$p_{\mu\nu}^{SCF}$	$r_{\mu\nu}^{SCF}$	$r_{\mu\nu}^{exp}$
p-Benzoquinone[b] (*I*)				3,10-Pyrenequinone (*V*)[f]			
A	0·9107	1·353	1·397	A	0·6241	1·405	1·320
B	0·3000	1·463	—	B	0·6741	1·396	1·442
C	0·8521	1·364	—	C	0·3550	1·453	1·420
1,4-Naphthoquinone (*II*)[c]				D	0·8848	1·358	1·380
A	0·9090	1·353	1·414	E	0·3392	1·456	—
B	0·3013	1·463	1·368	F	0·8268	1·368	—
C	0·8500	1·364	—	G	0·3175	1·460	—
D	0·3014	1·463	1·422	H	0·7089	1·389	—
E	0·6081	1·408	—	CH	0·5756	1·413	—
F	0·6491	1·400	—	I	0·5051	1·426	1·417
G	0·6570	1·399	—	J	0·5206	1·423	—
H	0·6695	1·396	—	K	0·5649	1·415	1·417
9,10-Anthraquinone (*III*)[d]				3,8-Pyrenequinone (*VI*)[f]			
A	0·5991	1·409	1·427	A	0·6002	1·409	1·320
B	0·3004	1·463	1·402	B	0·6914	1·393	1·442
C	0·8487	1·364	—	C	0·3528	1·453	1·420
D	0·6478	1·400	1·428	D	0·8868	1·357	1·380
E	0·6597	1·398	1·379	E	0·3369	1·456	—
F	0·6672	1·397	1·419	F	0·8260	1·368	—
9,10-Phenanthrenequinone (*IV*)[e]				G	0·3211	1·459	—
A	0·3065	1·462	1·448	H	0·6918	1·392	—
B	0·6020	1·409	1·404	I	0·5201	1·423	1·417
C	0·3136	1·461	1·390	J	0·5044	1·426	—
D	0·2384	1·474	1·372	K	0·5659	1·415	1·417
E	0·8679	1·361	—				
F	0·6371	1·402	1·457				
G	0·6691	1·397	1·381				
H	0·6585	1·398	1·398				
CH	0·6689	1·397	1·383				
I	0·3065	1·462	1·405				

[a] For designation of bonds see Scheme 1. [b] Lit.[51] (lit.[52]) gives the following values of $r_{\mu\nu}^{exp}$ for the quinone (in Å): bond A 1·32 (1·322), bond B 1·50 (1·477), bond C 1·14 (1·222). The data for the hydrocarbon, benzene, were taken from refs[53,54]. [c] The values of $r_{\mu\nu}^{exp}$ for naphthalene were taken from ref.[44]. [d] Lit.[55] records the following values of $r_{\mu\nu}^{exp}$ for the quinone (in Å): bond A 1·40, bond B 1·50, bond C 1·15, bond D 1·39, bond E 1·38 and bond F 1·38. The data for $r_{\mu\nu}^{exp}$ of the hydrocarbon, anthracene, were taken from ref.[44]. [e] The values of $r_{\mu\nu}^{exp}$ for phenanthrene were taken from ref.[56]. [f] The values of $r_{\mu\nu}^{exp}$ for pyrene were taken from ref.[57].

first $\pi\pi^*$ transition (at 29300 cm^{-1}) is symmetrically forbidden and corresponds to a moderately strong band at 36000 cm^{-1}. Also for the second absorption band predicted location is too red shifted (theory 36000 cm^{-1}, experiment 42000 cm^{-1}).

A better agreement was achieved with 1,4-naphthoquinone. For the region at 30000 cm^{-1} where a broad absorption band is located the theory predicts two strongly allowed transitions with the mutually perpendicular polatization directions, similarly as for the broad band at 40000 cm^{-1}. Polarization direction data are not available in the literature for this molecule. On analyzing the changes in the electronic spectra owing substitution Singh and coworkers[47] concluded that each of those both broad bands is composed from two perpendicularly polarized bands (indicated by arrows at maxima in Fig. 7), in agreement with the theoretical prediction.

It is apparent a satisfactory interpretation of the spectra of *para* quinones with an "outside" quinoid ring as *e.g.* 1,4-benzoquinone[48], 1,4-naphthoquinone, or 1,4-anthraquinone cannot be achieved without taking a strong C—C bond alternation in that ring into account.
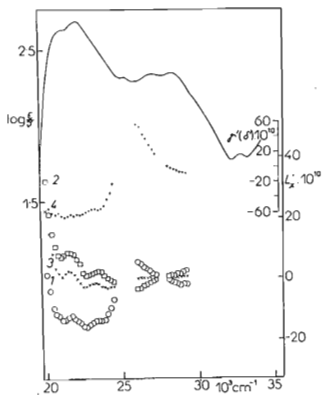

Fig. 12

Absorption Spectrum and Electrooptical Data on 3,10-Pyrenequinone in Dioxane
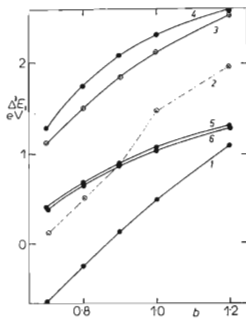
1, 2, 3, 4 see Fig. 11.

Fig. 13

Dependence of the First S–T Transition on Parameter b

1 *p*-Benzoquinone, 2 1,4-Naphthoquinone, 3 9,10-Anthraquinone, 4 9,10-Phenanthrenequinone, 5 3,10-Pyrenequinone, and 6 3,8-Pyrenequinone.

For 9,10-anthraquinone theory gives a good interpretation of the absorption curve. The first two $\pi\pi^*$ transitions are predicted very well, the third one satisfactorily, judging at the same time the agreement in energy, relative intensities and polarization directions[49,50]. In the light of arguments given in discussion of the spectra of 1,4-benzoquinone and 1,4-naphthoquinone this good agreement is not surprising. In 9,10-anthraquinone the bond alternation is considerably less than that in two preceding molecules, which is well reflected by the variable β approximation adopted. 9,10-phenanthrenequinone, the only *ortho* quinone in our series, represents a different structural type. In the theoretical treatment we used on purpose the same value of b (1·1) as in the preceding cases, regardless of the evident possibility to improve the agreement between theory and experiment by means of a lower value of b (Fig. 4). With b 1·1 the transition energies for all bands are considerably overestimated. For the first band the theoretical and experimental polarization direction are in agreement; for the region at $31\,000$ cm^{-1} the theory predicts two bands with the polarization directions perpendicular each to other. From the dichroitic measurements it appears there are indeed two perpendicularly polarized bands in that region, but their order is reversed when compared with that predicted by the theory. It should be mentioned, however, the experimental results for this region are not entirely convincing.

Peri-condensed quinones are represented in our series by two pyrenequinone isomers. The structure of each of them is of the completely different type when compared with that of the preceding quinones. Again, for the sake of comparison with other quinones we use the value b 1·1. For 3,10-pyrenequinone the theory overestimates a little the transition energy of the first band. The polarization direction determined from the dichroitic measurements agrees with the theoretical prediction. The agreement was found also for two bands with polarization directions perpendicular each to other in the region $25\,000-30\,000$ cm^{-1}. Owing to the low field effects found in the measurements, this assignment is not, however, entirely convincing. In the region $32\,000-30\,000$ cm^{-1} the absorption spectrum exhibits no clear-cut absorption, therefore any assignment of bands is impossible. Also in this case a better agreement between theory and experiment would be achieved by the adoption of lower b. The results of calculation for 3,8-pyrenequinone are in qualitative agreement with the experiment. In the region $20\,000-30\,000$ cm^{-1} there are probably at least two strongly overlapping bands. The shortwave region of the spectrum is again without a clear-cut absorption, which prevents from any band assignment.

Dependences of $p_{\mu\nu}^{\text{SCF}}$ on b (Figs 8, 9) have some common features: as b increases the C=O bond order becomes higher with all molecules while the bond orders of the C—C bonds adjacent to the C=O group (bonds with a nature of the single bond) become lower. The bond A in *p*-benzoquinone and 1,4-naphthoquinone has a considerable double bond nature, even more than the C=O bond, which is in disagreement with the experimental X-ray data (Table III). On contrary the bond order

for the bond A in 9,10-anthraquinone is close to the aromatic C—C bond order and is affected by b very little; this confirms a known experience that the nature of both outside rings in 9,10-anthraquinone is strongly aromatic. This was fully respected in our calculations, therefore the theory fits the experiment so well. With except of the C=O bond the bond lengths estimated from bond orders are in a good agreement with the experimental data[44] (Table III).

In 9,10-phenanthrenequinone the bonds C, D, A have a single bond nature, while the bond B of the aromatic nature is analogous to the bond A in 9,10-anthraquinone. Bond order of the "single" bonds decreases, as b increases, this decrease being significant for bonds C and D adjacent to the C=O bond but unimportant for the bond A.

All bonds of these molecules can be divided into three groups: bonds D (analogous to the A bond in 1,4-naphthoquinone) and F with a clear-cut double bond nature, the bonds C, E and G resembling single bonds and being similarly dependent on b as single bonds in 9,10-phenanthrenequinone, and bonds of an aromatic nature forming a slightly perturbated naphthalene subsystem. Fig. 13 presents the dependence of the first S—T transition on the parameter b (numerical results for b 1·1 are summarized in Table IV). It is noteworthy that differences in these transition energies are rather great with *para* quinones but very small for isomeric pyrenequinones.

REFERENCES

1. Namiot A. J., Djatkina M. E., Syrkin J. K.: Dokl. Akad. Nauk SSSR *48*, 267 (1945).
2. Pullman B., Pullman A.: *Les Théories Electroniques de la Chimie Organique.* Masson, Paris 1952.
3. Streitwieser A., jr: *Molecular Orbital Theory for Organic Chemists.* Wiley, New York 1961.
4. Koutecký J., Zahradník R., Arient J.: This Journal *27*, 2490 (1962).
5. Kon H.: Bull. Chem. Soc. Japan *28*, 275 (1955).
6. Leibovici C., Deschamps J.: Compt. Rend. *261*, 5487 (1965).
7. Kuboyama A., Wada K.: Bull. Chem. Soc. Japan *39*, 1874 (1966).
8. Leibovici C., Deschamps J.: Compt. Rend. *264*, 70 (1967).
9. Anno T., Matubara I., Sado A.: Bull. Chem. Soc. Japan *29*, 168 (1957).
10. Anno T., Sado A., Matubara I.: J. Chem. Phys. *26*, 967 (1957).
11. Anno T., Sado A.: Bull. Chem. Soc. Japan *31*, 728, 734 (1958).
12. Besnainou S., Bratož S.: J. Chem. Phys. *34*, 1142 (1961).
13. Leibovici C., Deschamps J.: Theoret. Chim. Acta (Berlin) *4*, 321 (1966).
14. Béry J. C.: J. Chim. Phys. *67*, 580 (1970).
15. Sandorfy C.: Can. J. Chem. *33*, 1337 (1955).
16. Yoshizumi H.: Trans. Faraday Soc. *53*, 125 (1957).
17. Hoffmann R.: J. Chem. Phys. *39*, 1397 (1963); *40*, 2745 (1964).
18. Yonezawa T., Yamabe H., Kato K.: Bull. Chem. Soc. Japan *42*, 76 (1969).
19. Leibovici C.: Anales Fís. *66*, 105 (1970).
20. Kunii T. L., Kuroda H.: Rep. Comp. Centre (University Tokyo) *1*, 119 (1968).
21. Nishimoto K., Forster L. S.: Theoret. Chim. Acta (Berlin) *3*, 407 (1965); *4*, 155 (1966).

22. Kunii T. L., Kuroda H.: Theoret. Chim. Acta (Berlin) *11*, 97 (1968).
23. Dewar M. J. S., Schmeising H. N.: Tetrahedron *5*, 166 (1959); *11*, 96 (1960).
24. Nishimoto K., Forster L. S.: J. Phys. Chem. *71*, 409 (1967); *72*, 914 (1968).
25. Kuroda H., Kunii T.: Theoret. Chim. Acta (Berlin) *7*, 220 (1967); *9*, 51 (1967).
26. *Tables of Interatomic Distances and Configuration in Molecules and Ions* (L. E. Sutton, Ed.). The Chemical Society, London 1958.
27. Trotter J.: Acta Cryst. *13*, 86 (1960).
28. Rees P. B.: Acta Cryst. *B 26*, 1292, 1298, 1304, 1311 (1970).
29. Allinger N. L., Freiberg L. A., Hermann R. B., Miller M. A.: J. Am. Chem. Soc. *85*, 1171 (1963).
30. Koutecký J.: Z. Physik. Chem. (Frankfurt) *52*, 8 (1967).
31. Hochmann P.: *Thesis*. Czechoslovak Academy of Sciences, Prague 1967.
32. Pariser R., Parr R. G.: J. Chem. Phys. *21*, 767 (1953).
33. Nishimoto K., Mataga N.: Z. Physik. Chem. (Frankfurt) *12*, 335 (1957); *13*, 140 (1957).
34. Organic Syntheses Vol. *34*, p. 76. Wiley, New York 1954.
35. Nepraš M.: Unpublished results.
36. *Laboratorní technika organické chemie* (B. Keil, Ed.). Published by Nakladatelství ČSAV, Prague 1963.
37. *UV Atlas Organischer Verbindungen*. Verlag Chemie, Berlin 1966.
38. Liptay W., Eberlein W., Weidenberg H., Elflein O.: Ber. *71*, 548 (1967).
39. Liptay W., Czekalla J.: Z. Naturforsch. *15a*, 1072 (1960).
40. Liptay W., Czekalla J.: Ber. *65*, 721 (1961).
41. Liptay W.: Z. Naturforsch. *20a*, 272 (1965).
42. Liptay W., Weisenberger H., Tiemann F., Eberlein W., Konopka G.: Z. Naturforsch. *23a*, 377 (1968).
43. Liptay W., Dumbacher B., Weisenberger H.: Z. Naturforsch. *23a*, 1602 (1968).
44. Golebiewski A., Nowakowski J.: Acta Phys. Polon. *25*, 647 (1964); *26*, 105 (1964).
45. Labhart H.: Chimia (Aarau) *15*, 20 (1961).
46. Caldwell C. C., LeFévre R. J. W.: J. Chem. Soc. *1939*, 1614.
47. Singh I., Ogata R. T., Moore E. E., Chang C. W. J., Scheuer P. J.: Tetrahedron *24*, 6053 (1968).
48. Klessinger M.: Theoret. Chim. Acta (Berlin) *5*, 251 (1966).
49. Popov K. R.: Optika i Spektroskopija *4*, 404 (1958).
50. Drotl H. R., Daarman H. H.: J. Chem. Phys. *47*, 1896 (1967).
51. Robertson J. M.: Proc. Roy. Soc. (London) *A 150*, 106 (1935).
52. Trotter J.: Acta Cryst. *13*, 86 (1960).
53. Stoicheff B. P.: Can. J. Phys. *32*, 339 (1954).
54. Langseth A., Stoicheff B. P.: Can. J. Phys. *34*, 350 (1956).
55. Sen S. N.: Indian J. Phys. *22*, 347 (1948).
56. Trotter J.: Acta Cryst. *16*, 605 (1963).
57. Camerman A., Trotter J.: Acta Cryst. *18*, 636 (1965).

Translated by P.Čársky.